

# Cosmology of Mass-Varying Neutrinos Driven by Quintessence: Theory and Observations

A. W. Brookfield,<sup>1</sup> C. van de Bruck,<sup>2</sup> D. F. Mota,<sup>3</sup> and D. Tocchini-Valentini<sup>4</sup>

<sup>1</sup>*Department of Applied Mathematics and Department of Physics,  
Astro-Particle Theory & Cosmology Group, Hounsfield Road,  
Hicks Building, University of Sheffield, Sheffield S3 7RH, United Kingdom*

<sup>2</sup>*Department of Applied Mathematics, Astro-Particle Theory & Cosmology Group,  
Hounsfield Road, Hicks Building, University of Sheffield, Sheffield S3 7RH, United Kingdom*

<sup>3</sup>*Institute of Theoretical Astrophysics, University of Oslo, 0315 Oslo, Norway*

<sup>4</sup>*Astrophysics Department, Oxford University, Keble Road, Oxford OX1 3RH, United Kingdom  
Department of Physics and Astronomy, The Johns Hopkins University, Baltimore, MD 21218, USA*

(Dated: 14 December 2005)

The effects of mass-varying neutrinos on cosmic microwave background (CMB) anisotropies and large scale structures (LSS) are studied. In these models, dark energy and neutrinos are coupled such that the neutrino masses are functions of the scalar field playing the role of dark energy. We begin by describing the cosmological background evolution of such a system. It is pointed out that, similar to models with a dark matter/dark energy interaction, the apparent equation of state measured with SNIa can be smaller than -1. We then discuss the effect of mass-varying neutrinos on the CMB anisotropies and the matter power spectrum. A suppression of power in the CMB power spectrum at large angular scales is usually observed. We give an explanation for this behaviour and discuss different couplings and quintessence potentials to show the generality of the results obtained. We perform a likelihood analysis using wide-ranging SNIa, CMB and LSS observations to assess whether such theories are viable. Treating the neutrino mass as a free parameter we find that the constraints on the coupling are weak, since CMB and LSS surveys give only upper bounds on the neutrino mass. However, fixing a priori the neutrino masses, we find that there is some evidence that the existence of such a coupling is actually preferred by current cosmological data over the standard  $\Lambda$ CDM cosmology.

PACS numbers: 98.80.-k, 98.80.Jk

Keywords: Cosmology: Theory, Large-Scale Structure of Universe

## I. INTRODUCTION

Recent cosmological observations indicate that the expansion of the universe is accelerating [1]-[3]. It follows from General Relativity that the dominant energy component today must have negative pressure. Many candidates have been proposed over the years, including scalar field models, which are well motivated from the point of view of particle physics theories, see e.g. [4]-[7]. The main prediction of these types of models is that the dark energy equation of state becomes a dynamical quantity, and can vary from the usual value of  $w = -1$  for a cosmological constant. Although such models are very attractive, they are plagued with several theoretical difficulties, such as the stability of the potential under quantum corrections [8] or why the dark energy scalar field seems not to mediate a force between normal matter particles [9]. In addition, the energy scale of the scalar field is put in by hand and usually not connected to a more fundamental energy scale. However, attempts have been made to address these problems, such as models with ultralight pseudo-Nambu-Goldstone bosons (see, for example, [10], [11] and [12]; for a review, see [13]).

It is expected that any explanation for dark energy will involve physics beyond the standard model of particle physics. Recently, a new class of models have been proposed, which entertain the idea of a possible connection

between neutrinos and dark energy. Their theoretical and observational consequences have already been studied very extensively [14]-[48]. The main motivation for a connection between dark energy and neutrinos is that the energy scale of dark energy ( $\mathcal{O}(10^{-3})$  eV) is of the order of the neutrino mass scale. In these models the neutrino mass scale and the dark energy scale are linked to each other, and hence the observed non-zero neutrino masses (see [49]-[51]) cannot be understood without an understanding of dark energy. Also, one may hope that these models might provide an explanation for the coincidence problem [18].

In this paper we investigate the cosmology of neutrino models of dark energy. We take into account the *full* evolution of the neutrinos, i.e. studying the relativistic and non-relativistic regimes and the transition in between.

Armed with a complete numerical model for the evolution of the coupled neutrinos, we compare the background evolution with Supernova data and study how the modified perturbations affect the cosmic microwave background radiation (CMB) temperature anisotropies and large scale structures (LSS) matter power spectrum. We thereby present the details of the results outlined in [28] and discuss other forms of coupling between dark energy and neutrinos and potentials for the dark energy field.

The paper is organized as follows: In Section II

we discuss the background evolution of the coupled dark energy–neutrino system in the context of a typical quintessential potential. In Section III we derive the evolution equations for cosmological perturbations in neutrino models of dark energy, and present the modified CMB and matter power spectra. In Section IV we discuss other couplings and potentials, such as inverse power-law potentials and field–dependent couplings. In Section V we compare our theory with data, using a public Markov-Chain Monte-Carlo data analysis program. We conclude in Section VI.

## II. THE COSMOLOGICAL BACKGROUND EVOLUTION

In a flat, homogeneous, Friedmann–Robertson–Walker universe with line-element

$$ds^2 = a^2(\tau) (-d\tau^2 + \delta_{ij} dx^i dx^j), \quad (1)$$

the Einstein equations describe the evolution of the scale factor  $a(\tau)$ :

$$H^2 \equiv \left(\frac{\dot{a}}{a}\right)^2 = \frac{8\pi}{3} G a^2 \rho, \quad (2)$$

$$\frac{d}{d\tau} \left(\frac{\dot{a}}{a}\right) = -\frac{4\pi}{3} G a^2 (\rho + 3p). \quad (3)$$

In these equations,  $\rho(\tau)$  and  $p(\tau)$  are the total energy density and pressure respectively and the dot refers to the derivative with respect to conformal time  $\tau$ . Defining  $\Omega_i = \rho_i/\rho_c$ , where  $\rho_c$  is the critical energy density for a flat universe and  $\rho_i$  are the energy densities of the individual matter species, the equations above require that  $\Omega = \sum_i \Omega_i = 1$ . In the following we will set  $8\pi G \equiv 1$ .

In our model we consider a universe with the usual energy–matter composition. At early times, the energy density is dominated by the relativistic species – radiation and highly relativistic neutrinos. As the universe expands the energy density in radiation decays, and the universe becomes matter dominated. The dominant matter species is assumed to be Cold Dark Matter (CDM), which is non–relativistic, weakly interacting and behaves like a perfect pressureless fluid. At this time there are also contributions to  $\Omega$  from baryons and neutrinos (which having cooled behave in a manner similar to CDM). At late times the matter energy densities also decay away, and we enter the dark energy dominated epoch. In common with standard quintessence models we describe the dark energy sector using a dynamical scalar field with potential  $V(\phi)$ , where the form of the potential is chosen (and fine–tuned) to produce the necessary late time acceleration. The energy density and pressure of the scalar field are defined by the usual expressions,

$$\rho_\phi = \frac{1}{2a^2} \dot{\phi}^2 + V(\phi) \quad (4)$$

$$p_\phi = \frac{1}{2a^2} \dot{\phi}^2 - V(\phi). \quad (5)$$

In this paper, we consider the consequences of a coupling between neutrinos and dark energy. To describe this coupling, we follow [18]: the coupling of dark energy to the neutrinos results in the neutrino mass becoming a function of the scalar field, i.e.  $m_\nu = m_\nu(\phi)$ , and so the mass of the neutrinos changes as the scalar field evolves. For our purposes it does not matter if the neutrinos are Majorana or Dirac particles, and for simplicity we assume three species of neutrinos with degenerate mass<sup>1</sup> It is well known [8] that the light mass of the quintessence potential results in it being highly unstable to radiative corrections, and that the addition of a coupling between the dark energy and other matter species only serves to further exacerbate this problem. In this regard it is important that both the quintessence potential and the neutrino mass are regarded as classical, effective quantities, which already include radiative corrections.

It is also important to note that our theory differs significantly in one key aspect from the work of [18]. In our models, the dark energy sector is described by a *light* scalar field, with a mass which is at most of order  $H$ . The potential chosen by Fardon et al. was such that the mass of the scalar field is much larger than  $H$  for most of its history, and this can have significant implications upon the behaviour of the neutrino background and the growth of perturbations [33] as we will discuss later.

To fully describe the evolution of cosmological neutrinos, we must calculate their distribution function  $f(x^i, p^i, \tau)$  in phase space. An important fact to note is that even though the neutrinos interact with dark energy, we treat the interaction classically and, as will be shown in eq. (22), they can be thought as free-falling in a metric given by

$$g_{\alpha\beta}^\nu = m_\nu(\phi)^2 g_{\alpha\beta}. \quad (6)$$

Thus, the theory we are going to consider is a special type of scalar-tensor theory, in which the scalar degree of freedom couples only to neutrinos. It follows that the neutrino phase-space density is incompressible and we can treat the neutrinos as collisionless particles throughout the period of interest as long as we keep track of the evolution of the neutrino mass. We therefore need to solve the Boltzmann equation in collisionless form simultaneously with the scalar field evolution equations. Once the distribution function is known, the pressure and energy density of the neutrinos can be calculated. In this Section we will discuss the background evolution only; in the next Section we will discuss cosmological perturbations in these models.

---

<sup>1</sup> In fact, such an assumption is quite natural and has no strong consequences to this work. In the mass regions detectable in astronomical observations, the three neutrino masses are nearly degenerate. Adding to that, cosmology is in leading order sensitive to  $\sum m_\nu$ .

The energy density stored in the neutrinos is given by

$$\rho_\nu = \frac{1}{a^4} \int q^2 dq d\Omega \epsilon f_0(q), \quad (7)$$

and the pressure by

$$p_\nu = \frac{1}{3a^4} \int q^2 dq d\Omega f_0(q) \frac{q^2}{\epsilon}, \quad (8)$$

where  $f_0(q)$  is the usual unperturbed background neutrino Fermi-Dirac distribution function

$$f_0(\epsilon) = \frac{g_s}{h_P^3} \frac{1}{e^{\epsilon/k_B T_0} + 1}, \quad (9)$$

and  $\epsilon^2 = q^2 + m_\nu^2(\phi)a^2$  ( $q$  denotes the comoving momentum). As usual,  $g_s$ ,  $h_P$  and  $k_B$  stand for the number of spin degrees of freedom, Planck's constant and Boltzmann's constant respectively. In the following we will assume that the neutrinos decouple whilst they are still relativistic, and therefore the phase-space density only depends upon the comoving momentum. Taking the time-derivative of eq. (7), it can be easily shown that

$$\dot{\rho}_\nu + 3H(\rho_\nu + p_\nu) = \frac{d \ln m_\nu}{d\phi} \dot{\phi} (\rho_\nu - 3p_\nu). \quad (10)$$

We describe the dark energy sector using a scalar field with potential  $V(\phi)$ . Taking into account the energy conservation of the coupled neutrino–dark energy system, one can immediately find that the evolution of the scalar field is described by a modified Klein-Gordon equation

$$\ddot{\phi} + 2H\dot{\phi} + a^2 \frac{dV}{d\phi} = -a^2 \frac{d \ln m_\nu}{d\phi} (\rho_\nu - 3p_\nu). \quad (11)$$

This equation contains an extra source term with respect to the uncoupled case, which accounts for the energy exchange between the neutrinos and the scalar field.

For the remainder of this Section and the next, we consider a typical exponential form for the dark energy potential, namely

$$V(\phi) = V_0 e^{-\sigma\phi} \quad (12)$$

and define  $\sigma \equiv \sqrt{\frac{3}{2}}\lambda$ . We also choose to take

$$m_\nu(\phi) = M_0 e^{\beta\phi} \quad (13)$$

The exponential potential can produce a non-scaling solution that may give late time acceleration, depending upon the steepness of the potential,  $\sigma$  (see e.g. [34, 35, 36, 37, 52]). In an uncoupled system with  $\sigma < \sqrt{6}$  there exists a critical point that is stable for  $\sigma^2 < 3(1+w)$ , where  $w$  stands for the equation of state of matter or radiation, and in which  $\Omega_\phi = 1$ . This solution will lead to acceleration provided that  $\sigma < \sqrt{2}$ . The existence of scaling solutions depends upon the equation of state of the other components present in the universe. Choosing

$\sigma^2 > 3(1+w)$  leads to a scaling solution with  $\Omega_\phi = 3(1+w)/\sigma^2$  [34]. (See also [53], who use the exponential potential as a dark energy model.) The requirement that the present day dark energy density is  $\Omega_\phi \sim 0.7$  is hard to reconcile with the scaling solution at early times, since in this case it follows that  $\Omega_\phi = 4/\sigma^2$ , whilst big bang nucleosynthesis requires that the dark energy density in the early universe is very small [38].

In this Section we focus our discussion on models with  $\sigma < \sqrt{2}$ , which with an appropriate choice of  $V_0$ , can provide late-time acceleration with  $\Omega_\phi \sim 0.7$  today (note that the late-time attractor  $\Omega_\phi = 1$  lies in the future). This choice of  $\sigma$  also ensures that the energy density in the form of dark energy at the time of BBN is very small, because for early times the quintessence field is frozen and acts like a cosmological constant with an energy density similar to the observed dark energy density today.

The presence of neutrino coupling can potentially affect this result, as the coupled field begins to evolve at earlier redshifts ( $z \sim 10^7$ ), however the fraction of the total energy stored in the scalar field at early times remains insignificant. Note that this choice of potential reduces to the cosmological constant case for a perfectly flat potential with zero coupling.

From the neutrino energy conservation equation (10), and for our choice of  $m_\nu(\phi)$  and  $V(\phi)$ , one can see that the dynamics of the scalar field can be described by an *effective potential*

$$V_{\text{eff}} = V(\phi) + (\tilde{\rho}_\nu - 3\tilde{p}_\nu) e^{\beta\phi}, \quad (14)$$

where  $\tilde{\rho}_\nu \equiv \rho_\nu e^{-\beta\phi}$  and  $\tilde{p}_\nu \equiv p_\nu e^{-\beta\phi}$  are independent of  $\phi$ . It can be shown that the effective potential will only have a minimum when  $\beta\sigma > 0$ . For the neutrinos we have numerically evaluated the integrals (7) and (8), which then have been used in the Klein-Gordon eq. (11) to find the evolution of the scalar field.

Figure 1 shows some typical examples of how the coupling of the neutrinos to the scalar field causes the mass of the neutrinos to evolve with time. Deep within the radiation dominated epoch, at times when the neutrinos are highly relativistic, the scalar field is Hubble damped and therefore the neutrino mass is (almost) constant. For quintessence models,  $\dot{\phi}$  is at most of order  $H$ , and therefore for relativistic species the coupling term in equation (10) is clearly suppressed relative to the Hubble damping term. As the universe expands the neutrinos cool and become non-relativistic at a temperature corresponding to the neutrino mass. Hence, the extra coupling terms in equations (10) and (11) become more and more important, allowing energy to be exchanged between the neutrinos and the scalar field. This interaction causes the scalar field, and hence the neutrino mass, to evolve.

It is important to note the two different types of behaviour seen in Figure 1 for the evolution of the neutrino mass. For models which have  $\beta\sigma > 0$  the effective potential possesses a minimum, and after some time the field passes through this minimum, slows down, stops and eventually rolls back towards the minimum. For models

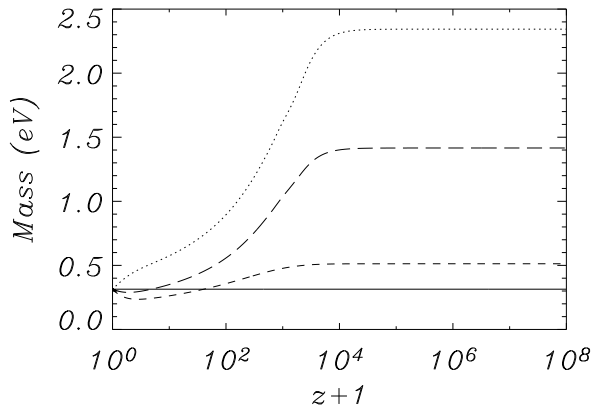


FIG. 1: Plot showing the evolution of the neutrino mass for an exponential potential and coupling (solid line:  $\beta = 0$ ,  $\lambda = 1$ ; short dashed line:  $\beta = 1$ ,  $\lambda = 1$ ; dotted line:  $\beta = -0.79$ ,  $\lambda = 1$ ; long dashed line  $\beta = 1$ ,  $\lambda = 0.5$ ). In all models, we have arranged that  $m_\nu = 0.314$  eV today.

which do not possess an effective minimum  $\dot{\phi}$  is always negative, and the scalar field will continue to roll down the effective potential unimpeded. We compare the behaviour of our light scalar field with the heavy acceleration field used in [18] - in their model the scalar field sits in the effective minimum of its potential for most of the time during the cosmic history, and it is the evolution of the effective minimum which drives the dynamics of the neutrino mass. As discussed in [18], the mass of their neutrinos increases as the universe expands, whereas in our model the neutrinos are heavier in the past and become lighter (although as we will discuss in Section IV, suitable choices of coupling and potential can realize coupled neutrino-quintessence models with neutrinos which are lighter in the past).

For the model described in this section the coupled neutrinos are heavier in the past than uncoupled neutrinos, which implies that the energy density stored in the neutrinos is larger than would normally be expected. This means that the evolution of the neutrino density parameter  $\Omega_\nu$  depends on the evolution of the neutrino mass, which in turn depends on the choice of the coupling  $\beta$  and the slope of the potential  $\sigma$ . This can be seen from Figure 2. The coupling of neutrinos to dark energy significantly alters the evolution of the cosmological background. In particular it can be seen that the extra energy stored in the neutrinos in the past can alter the redshift of matter-radiation equality.

Typically one expects non-relativistic neutrinos to behave in a similar manner to CDM, however the interaction between the neutrinos and the scalar field modifies the scaling behaviour of the non-relativistic neutrinos. It can be seen that the neutrino energy density dilutes away faster than that of CDM, which is especially notable for large values of coupling. The evolution of  $\phi$  caused

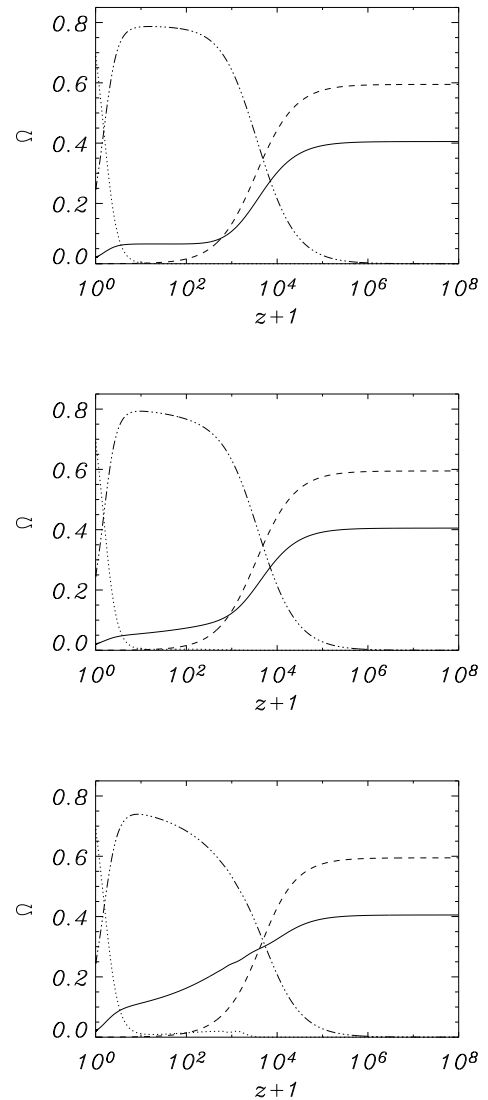


FIG. 2: Background evolution: In the upper panel, we plot the evolution of the density parameters for a model with  $\beta = 0$ ,  $\lambda = 1$ . In the middle panel the corresponding plot with  $\beta = 1$  is shown, whilst the lower plot shows the case  $\beta = -0.79$ ,  $\lambda = 1$ . (Neutrinos: solid line, CDM: dot-dashed line, scalar field: dotted line and radiation: dashed line.) In all cases, the mass of the neutrinos is  $m_\nu = 0.314$  eV today. We consider a flat universe with  $\Omega_b h^2 = 0.022$ ,  $\Omega_c h^2 = 0.12$ ,  $\Omega_\nu h^2 = 0.01$  and  $h = 0.7$ .

by the transfer of energy between the coupled neutrinos and scalar field also results in the energy density of the quintessence field becoming dominated by kinetic energy. Finally at a redshift of the order of unity the potential energy of the scalar field begins to dominate, and all other matter species decay away.

A final point we would like to raise is the fact the *apparent* equation of state measured by an observer is

not given by

$$w_\phi = \frac{p_\phi}{\rho_\phi}, \quad (15)$$

where  $\rho_\phi$  and  $p_\phi$  are defined in eqns (4) and (5). One of the usual assumptions made in the measurements of the dark energy equation of state using supernovae is that matter (dark, baryonic or neutrinos) is decoupled from dark energy. At low redshifts, all these components are assumed to scale like  $a^{-3}$ . This is clearly not the case with the coupled neutrinos here. It was pointed out in [54], that the apparent equation of state is given by<sup>2</sup>

$$w_{\text{ap}} = \frac{w_\phi}{1-x}, \quad (16)$$

with

$$x = -\frac{\rho_{\nu,0}}{a^3 \rho_\phi} \left[ \frac{m_\nu(\phi)}{m_\nu(\phi_0)} - 1 \right]. \quad (17)$$

In this equation, the subscript 0 denotes the quantities at the present epoch. We emphasise that this quantity is *not* the effective equation of state of dark energy, which is defined as

$$\dot{\rho}_\phi + 3H\rho_\phi(1+w_{\text{eff}}) = 0, \quad (18)$$

while assuming that the neutrino density and neutrino pressure evolve according to Eq. (10). Using the Klein-Gordon equation, one finds that the effective equation of state can be written as

$$w_{\text{eff}} = w_\phi + \frac{\beta \dot{\phi}}{3H} \frac{\rho_\nu}{\rho_\phi}. \quad (19)$$

In Fig. 3, we plot the apparent equation of state  $w_{\text{ap}}$  as a function of redshift. Note that  $w_{\text{ap}}$  can be less than  $-1$ , as was pointed out in [55], [56] and [54] in the context of models with dark matter/dark energy interaction.

To conclude this part, even if dark energy couples only to a subdominant component such as neutrinos, the apparent equation of state can be less than  $-1$ , without introducing phantom fields. As it can be seen from Figure 3, the apparent equation of state might even cross the boundary  $w = -1$ .

### III. PERTURBATION EVOLUTION

Let us now turn our attention to the evolution of cosmological perturbations in our model. We adopt the conventions of Ma and Bertschinger [57] and work in the synchronous gauge, taking the line element to be

$$ds^2 = -a^2 d\tau^2 + a^2 (\delta_{ij} + h_{ij}) dx^i dx^j. \quad (20)$$

<sup>2</sup> The authors of [54] called this quantity an effective equation of state. However, we will define an effective equation of state below.

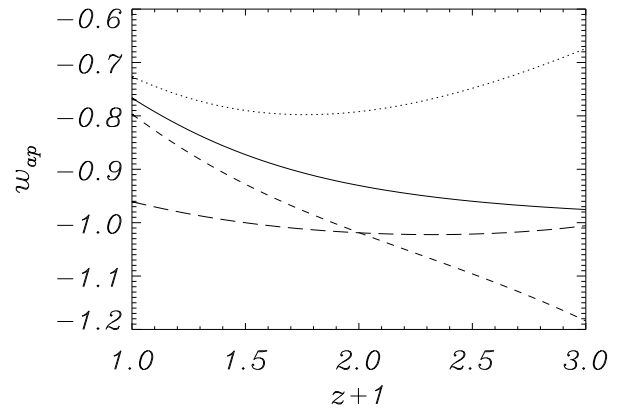


FIG. 3: The apparent equation of state, as defined in eq. (16), as a function of redshift  $z$  (solid line:  $\beta = 0$ ,  $\lambda = 1$ ; short dashed line:  $\beta = 1$ ,  $\lambda = 1$ ; dotted line:  $\beta = -0.79$ ,  $\lambda = 1$ ; long dashed line  $\beta = 1$ ,  $\lambda = 0.5$ .)

(For a review of cosmological perturbation theory, see [58], [59] or [60].)

As already mentioned in the last section, to fully describe the evolution of cosmological neutrinos, we must calculate their distribution function  $f(x^i, p^i, \tau)$  in phase space. We can treat the neutrinos as collisionless particles throughout the period of interest, and hence we can find the neutrino distribution function by solving the collisionless Boltzmann equation [57]

$$\frac{\partial f}{\partial \tau} + \frac{dx^i}{d\tau} \frac{\partial f}{\partial x^i} + \frac{dq}{d\tau} \frac{\partial f}{\partial q} + \frac{dn^i}{d\tau} \frac{\partial f}{\partial n^i} = 0, \quad (21)$$

where the comoving momentum is  $q_i = ap_i$ . It is convenient to rewrite the comoving momentum in terms of its magnitude and direction:  $q^i = qn^i$ . The last term in equation (21) is a second order quantity and will be neglected in the following linear perturbation formalism.

The path of a neutrino in spacetime is governed by the general action

$$S = - \int m_\nu(\phi) \sqrt{-ds^2}, \quad (22)$$

which can be minimised to derive the neutrino geodesic equation<sup>3</sup>

$$P^0 \frac{\partial P^\rho}{\partial \tau} + \Gamma_{\alpha\beta}^\rho P^\alpha P^\beta = -m_\nu^2 \frac{d \ln m_\nu}{d\phi} \frac{\partial \phi}{\partial x_\rho}, \quad (23)$$

where  $P^\mu$  is the proper momentum of the neutrino. Taking the zeroth component of this equation and using the

<sup>3</sup> Please note Errata at the end of this paper.

relation  $P^0 = \epsilon a^{-2}$ , one finds that the comoving three-momentum of the neutrinos is given by<sup>3</sup>

$$\frac{dq}{d\tau} = -\frac{1}{2}q\dot{h}_{ij}n_in_j. \quad (24)$$

This equation does not depend explicitly on the coupling or the scalar field perturbations. Following [57], we write the phase space distribution of the neutrinos as a zeroth order distribution plus a small perturbation

$$f(x^i, p_j, \tau) = f_0(q) [1 + \Psi(x^i, q, n_j, \tau)]. \quad (25)$$

Substituting this expression into the Boltzmann equation and performing a Fourier transformation, we find<sup>3</sup>

$$\begin{aligned} \frac{\partial \Psi}{\partial \tau} + i\frac{q}{\epsilon}(\mathbf{k} \cdot \mathbf{n})\Psi \\ + \frac{d \ln f_0}{d \ln q} \left[ \dot{\eta} - \frac{\dot{h} + 6\dot{\eta}}{2}(\mathbf{k} \cdot \mathbf{n})^2 \right] = 0 \end{aligned} \quad (26)$$

In this equation (and in eqs. (29) and (31), given later),  $\eta$  and  $h$  are the standard scalar parts of the metric perturbation  $h_{ij}$ . It is clear that equation (26) does not contain terms proportional to  $d \ln m_\nu / d\phi$ . Therefore, the equations for the neutrino hierarchy derived in [57] do not change<sup>3</sup>. However, the expressions for the perturbed neutrino energy density and neutrino pressure, which will be calculated using  $f$ , are modified. The perturbed energy density is given by

$$\delta\rho_\nu = \frac{1}{a^4} \int q^2 dq d\Omega f_0 \left( \epsilon\Psi + \frac{d \ln m_\nu}{d\phi} \frac{m_\nu^2 a^2}{\epsilon} \delta\phi \right) \quad (27)$$

which can be written as

$$\delta\rho_\nu = \frac{1}{a^4} \int q^2 dq d\Omega \epsilon f_0(q) \Psi + \delta\phi \frac{d \ln m_\nu}{d\phi} (\rho_\nu - 3p_\nu). \quad (28)$$

Similarly, the expression for the perturbation in the neutrino pressure is given by

$$\delta p_\nu = \frac{1}{3a^4} \int q^2 dq d\Omega f_0(q) \left( \frac{q^2}{\epsilon} \Psi - \delta\phi \frac{d \ln m_\nu}{d\phi} \frac{q^2 m_\nu^2 a^2}{\epsilon^3} \right).$$

The expressions for the neutrino shear and energy flux remain unchanged as they do not depend explicitly upon  $m_\nu$ . Finally, the perturbed Klein-Gordon equation is given by:

$$\begin{aligned} \delta\ddot{\phi} + 2H\delta\dot{\phi} + \left( k^2 + a^2 \frac{d^2 V}{d\phi^2} \right) \delta\phi + \frac{1}{2}\dot{h}\dot{\phi} = \\ -a^2 \left[ \frac{d \ln m_\nu}{d\phi} (\delta\rho_\nu - 3\delta p_\nu) + \frac{d^2 \ln m_\nu}{d\phi^2} \delta\phi (\rho_\nu - 3p_\nu) \right]. \end{aligned} \quad (29)$$

To calculate the temperature anisotropy spectrum and matter power spectrum we apply these modifications to CAMB [61]. This code calculates the linear cosmic background anisotropy spectra by solving the Boltzmann

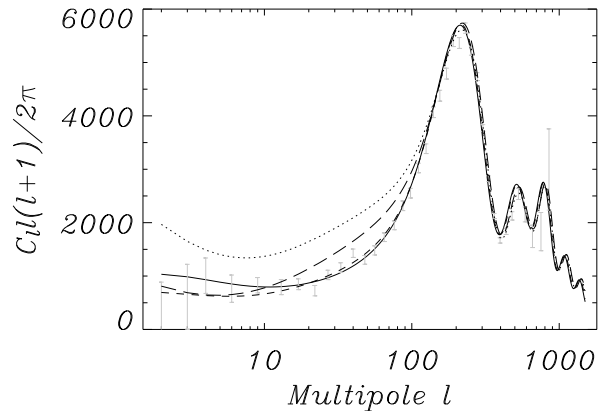


FIG. 4: The CMB anisotropy spectrum (unnormalized) for exponential coupling and potential. Solid line:  $\beta = 0$ ,  $\lambda = 1$ ; short-dashed line:  $\beta = 1$ ,  $\lambda = 1$ ; dotted line:  $\beta = -0.79$ ,  $\lambda = 1$ ; long-dashed line:  $\beta = 1$ ,  $\lambda = 0.5$ . Error bars denote WMAP data.

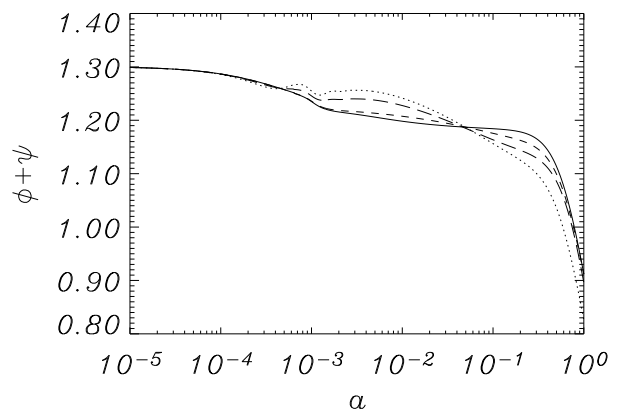


FIG. 5: Evolution of the sum of the metric perturbations  $\Phi + \Psi$ . Solid line:  $\beta = 0$ ,  $\lambda = 1$ ; short-dashed line:  $\beta = 1$ ,  $\lambda = 1$ ; dotted line:  $\beta = -0.70$ ,  $\lambda = 1$ ; long-dashed line:  $\beta = 1$ ,  $\lambda = 0.5$ . The scale is  $k = 10^{-3} \text{Mpc}^{-1}$ .

equation which governs the evolution of the density perturbations, and integrating the sources along the photon past light cone. To ensure the accuracy of our calculations, we directly integrate the neutrino distribution function, rather than using the standard velocity weighted series approximation scheme. We do not consider lensing effects, nor tensor contributions.

The results of the neutrino-dark energy coupling on the temperature anisotropy spectrum can be seen in Figure 4. The most obvious modifications to the anisotropy spectrum occur for large angular scales, with  $\ell < 100$ , although for some choices of parameters the positions and relative heights of the peaks are also affected. We gener-

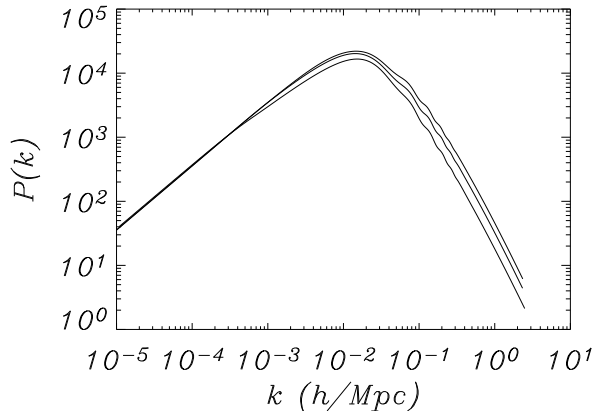


FIG. 6: Plot of the matter power spectrum. From the top curve to the bottom curve:  $(\beta = 0, \lambda = 1)$ ,  $(\beta = 1, \lambda = 0.5)$ ,  $(\beta = -0.79, \lambda = 1)$ . The matter power spectrum for  $(\beta = 1, \lambda = 1)$  is indistinguishable from the  $(\beta = 0, \lambda = 1)$  curve.

ally observe an increase in power for  $10 < \ell < 100$ , whilst for  $\ell < 10$  we find either an excess or reduction in power depending upon our choice of parameters. Note that this is in marked contrast to models of coupled CDM, where an increase in power on large scales is usually observed [62]. For the models where the neutrinos were much heavier in the past than today, we also observe a slight shift in the acoustic peaks and a change in their relative amplitudes.

For scales larger than a degree ( $\ell < 100$ ), the dominant contribution to the anisotropy spectrum is the Integrated Sachs-Wolfe Effect (IWS). This arises due to the evolution of the gravitational potentials along the photon path from the surface of last scattering. The modification to the cosmological background arising from the neutrino coupling can have a significant effect upon the evolution of the perturbations. In particular there is a larger energy density in neutrinos in coupled models during the transition period when the neutrinos become non-relativistic. As a result, the intermediate regime between radiation and matter domination is prolonged, and so the evolution of the gravitational potentials are significantly modified. The evolution of the sum of the metric perturbations  $\Phi$  and  $\Psi$  is shown in Figure 5. The modifications to the behaviour of the metric perturbations for the different models is immediately apparent.

For very large scales ( $\ell \leq 20$ ) anisotropies arise primarily from the late time Integrated Sachs-Wolfe effect (ISW), which is caused by the evolution of the metric perturbations for redshifts in the range  $0 < z < 2$ . In particular,  $\rho_\phi$  and  $\rho_\nu$  as well as the equation of state of dark energy affect the late time behaviour of cosmological perturbations. As mentioned above, the evolution of the scalar field is influenced by the presence of the coupling to the neutrinos and hence the equation of state of dark energy depends upon  $\beta$ . Likewise, the clustering prop-

erties of dark energy depends on the neutrino coupling (see [63] for a discussion on the clustering of dark energy and its impact on the CMB). The neutrinos will generally tend to fall into the potential wells of dark matter, although at a rate slightly dependent on the coupling to the scalar field. The scalar field itself will cluster together with the neutrinos and thereby affecting the gravitational potential.

Let us turn our discussion to the evolution of neutrino perturbations. Figure 6 shows the effects of neutrino coupling on the matter power spectrum. Here we typically observe damping, and our results appear similar to standard models of CDM and hot dark matter, where a similar reduction in power could be achieved with a heavier neutrino mass.

We can use the perturbed part of the energy momentum conservation equation for the coupled neutrinos

$$T^\mu{}_{\gamma;\mu} = \frac{d \ln m_\nu}{d\phi} \phi_{,\gamma} T^\alpha{}_\alpha \quad (30)$$

to calculate the evolution equations for the neutrino perturbations ( $T^\alpha{}_\alpha$  stands for the trace of the neutrino energy momentum tensor and the semicolon denotes the covariant derivative). Taking  $\gamma = 0$  we derive the equation governing the evolution of the neutrino density contrast,  $\delta_\nu \equiv \frac{\delta \rho_\nu}{\rho_\nu}$  whilst taking  $\gamma = i$  (spatial index) yields the velocity perturbation equation  $\theta_\nu \equiv ik_i v_\nu^i$ , with the coordinate velocity  $v_\nu^i \equiv dx^i/d\tau$ :

$$\begin{aligned} \dot{\delta}_\nu &= 3 \left( H + \beta \dot{\phi} \right) \left( w_\nu - \frac{\delta p_\nu}{\delta \rho_\nu} \right) \delta_\nu - (1 + w_\nu) \left( \theta_\nu + \frac{\dot{h}}{2} \right) \\ &+ \beta (1 - 3w_\nu) \dot{\delta}\phi + \frac{d\beta}{d\phi} \dot{\phi} \delta\phi (1 - 3w_\nu), \end{aligned} \quad (31)$$

$$\begin{aligned} \dot{\theta}_\nu &= -H(1 - 3w_\nu)\theta_\nu - \frac{\dot{w}_\nu}{1 + w_\nu} \theta_\nu + \frac{\delta p_\nu / \delta \rho_\nu}{1 + w_\nu} k^2 \delta_\nu \\ &+ \beta \frac{1 - 3w_\nu}{1 + w_\nu} k^2 \delta\phi - \beta(1 - 3w_\nu) \dot{\phi} \theta_\nu - k^2 \sigma_\nu. \end{aligned} \quad (32)$$

The variable  $\sigma_\nu$  represents the neutrino anisotropic stress and we have used the more general definition  $\beta = d \ln m_\nu / d\phi$ , which in general might be not constant. Furthermore the neutrino equation of state is given by  $w_\nu \equiv p_\nu / \rho_\nu$ .

It is the presence of the additional coupling terms in these expressions for the growth of the neutrino density and velocity perturbations, as well as the modifications to the evolution of the cosmological background, which alters the behaviour of the neutrino perturbations in comparison with the standard uncoupled case.

Figure 7 shows the evolution of the neutrino and CDM density contrasts, comparing the uncoupled model with an extreme coupled case with  $\beta = -0.79$ , for which the mass of the neutrinos is  $m_\nu \approx 2.5$  eV at  $z \geq 1400$  but  $m_\nu = 0.3$  eV today. Deep inside the radiation dominated epoch the neutrinos are highly relativistic and their density contrast grows in a similar manner to radiation. In

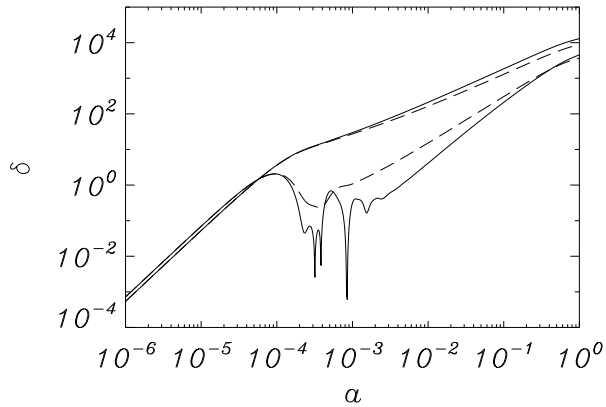


FIG. 7: Evolution of the neutrino (lower curves) and CDM (upper curves) density contrasts. The solid line shows the uncoupled case, i.e.  $\beta = 0$ , whereas the dashed line shows the case for  $\beta = -0.79$ . The scale is  $k = 0.1\text{Mpc}^{-1}$ .

the uncoupled models the growth of the density perturbations of the neutrinos makes a transition to matter-like behaviour once the neutrinos become non-relativistic. The neutrinos will fall into the CDM potential wells, which is the dominant component at recombination. At small wavelengths (large wavenumbers), the neutrinos undergo freestreaming, which prevents neutrinos from clustering at an arbitrary small scale. The freestreaming length scale after the neutrinos become non-relativistic can be estimated to be [57] (reinstating Newton's constant  $G$ )

$$k_{\text{fs}}(a) = \frac{4\pi G \rho a^2}{v_{\text{med}}^2} \quad (33)$$

where  $\rho$  is the background total density. The median neutrino speed is given by:

$$v_{\text{med}} = 15a^{-1} \left( \frac{m_\nu(a)}{10 \text{ eV}} \right) \text{ km s}^{-1}. \quad (34)$$

Since the neutrino momentum decays like  $a^{-1}$ , the neutrino velocity behaves like  $(am_\nu(a))^{-1}$ , taking into account that the neutrino mass evolves with time. Freestreaming stops as soon as  $k < k_{\text{fs}}$ , allowing the neutrino density contrast to grow. This behaviour can clearly be seen in Figure 7 for both the uncoupled and coupled cases. At around  $z \approx 10^4$  the neutrinos become non-relativistic and start to freestream immediately, as can be seen from the oscillating behaviour of  $\delta_\nu$ . At this stage  $k_{\text{fs}} < k$ . However, as soon as  $k_{\text{fs}} = k$  freestreaming stops, and  $\delta_\nu$  can grow unimpeded. The case with neutrino-dark energy coupling differs from the uncoupled case since in the result shown the neutrinos are heavier in the past, so for a given redshift  $k_{\text{fs}}$  is larger. This means that freestreaming stops earlier than in the uncoupled case. This behaviour is apparent in Figure 7 (dashed

lines), where we see that  $\delta_\nu$  starts to grow earlier than in the uncoupled case (solid lines). The neutrino-coupling also has an effect on the growth of the density contrast itself since we observe that  $\delta_\nu$  grows slower than in the uncoupled case. This is probably because the rate of gravitational infall of the neutrinos tends to be reduced by the presence of the much less clustered dark energy. Also, the coupling has a slight effect on the growth of the dark matter density contrast, which arises from the fact that the background evolution is modified.

#### IV. ANOTHER CHOICE OF COUPLING AND POTENTIAL

So far we have restricted our discussion to one choice of quintessence–neutrino coupling and one form for the dark energy potential. At this stage, the reader might wonder whether the results obtained so far are simply due to our choice of potential and coupling. For a scalar field with standard kinetic term, the exponential potential is not a favored model for a quintessential potential, since the initial value of the scalar field has to be fine-tuned to obtain scalar field domination today [64]. The interesting alternative possibility of a global attractor unfortunately does not seem to be viable due to the large perturbation growth [62]. The coupling of the scalar field to neutrinos does not cure the fine-tuning problem of the exponential potential.

For our second form of coupling we choose

$$m_\nu(\phi) = M_0 e^{\beta\phi^2}, \quad (35)$$

which was also recently used in a model with dark matter/dark energy coupling in [65]. The effect of this choice is that the coupling function  $d \ln m_\nu / d\phi$  becomes *field-dependent*, whereas it has been constant so far. Depending on how the field evolves with time, the coupling can either grow or become smaller during the cosmic history. Field-dependent couplings are not uncommon in higher-dimensional theories and can appear in brane-world theories, see for example [66] or [67].

For the potential, we choose an inverse power-law potential, which is a well-motivated candidate for a quintessence field (see e.g. [68] and [69]). To be concrete, we use

$$V(\phi) = \frac{M^6}{\phi^2}. \quad (36)$$

With these choices for the potential and coupling, the effective minimum will exist if  $\beta > 0$ .

The results for the neutrino-mass evolution, the apparent equation of state and the CMB anisotropy power-spectrum are shown in Figures 8, 9 and 10.

The biggest difference to the case of a purely exponential coupling is that for positive  $\beta$  the neutrinos are lighter in the past, as can be seen from Figure 8. Thus, with a convenient choice of potential and coupling, the



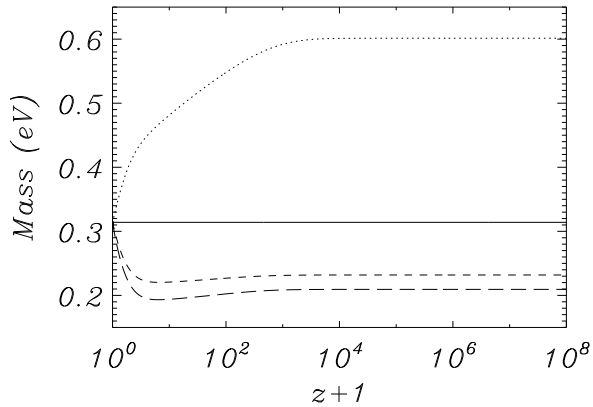


FIG. 8: The evolution of the neutrino mass for the inverse power-law potential with  $m_\nu(\phi) = m_0 e^{\beta\phi^2}$  (solid line:  $\beta = 0$ ; short dashed line:  $\beta = 0.2$ ; dotted line:  $\beta = -0.2$ ; long dashed line  $\beta = 0.27$ .)

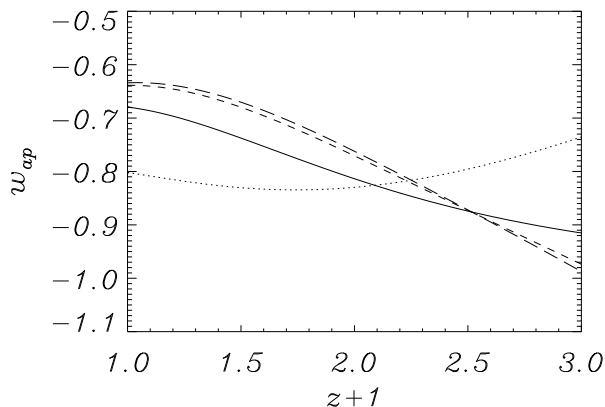


FIG. 9: The evolution of the apparent dark energy equation of state for the inverse power-law potential with  $m_\nu(\phi) = m_0 e^{\beta\phi^2}$  (solid line:  $\beta = 0$ ; short dashed line:  $\beta = 0.2$ ; dotted line:  $\beta = -0.2$ ; long dashed line  $\beta = 0.27$ .)

neutrinos can become heavier as the universe expands. In the case of a negative  $\beta$ , the effective potential does not have a minimum and the neutrinos become lighter as the universe expands. The results for the apparent equation of state are shown in Figure 9. The results are similar to the ones found in Section II:  $w_{\text{ap}}$  can be smaller than  $-1$  and can cross the boundary of the cosmological constant with  $w = -1$ . As it can be seen in Figure 9, the apparent equation of state varies substantially in the redshift range  $z = 0 - 2$  if  $\beta$  is non-zero. A strongly, however, varying equation of state is not preferred by the data. Finally, the effects on the CMB anisotropies are similar to the ones found in Section III, as can be seen from Figure 10. The only visible deviation from  $\beta = 0$  is the case

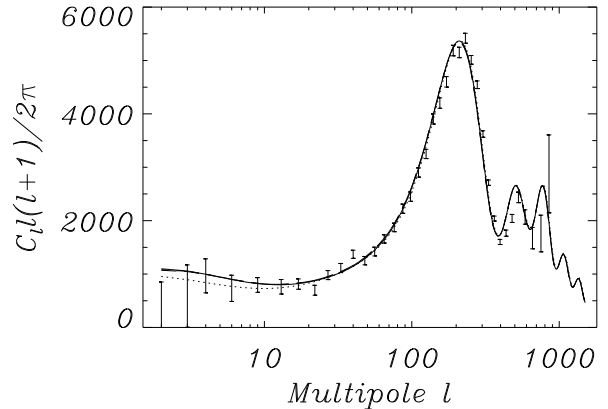


FIG. 10: The CMB anisotropy spectrum (unnormalized) for an exponential potential and  $m_\nu(\phi) = m_0 e^{\beta\phi^2}$  (solid line:  $\beta = 0$ ; short dashed line:  $\beta = 0.2$ ; dotted line:  $\beta = -0.2$ ; long dashed line  $\beta = 0.27$ .)

with negative  $\beta$ , in which a reduction of power at low multipoles can be observed. The cases with positive  $\beta$  can not be distinguished from the uncoupled case. The reason is that the neutrino density is smaller in the past than in the uncoupled case for this choice of potential and coupling. Hence, neutrinos are less important for the dynamics of the universe, and their imprint upon the CMB is correspondingly reduced.

In essence, the physical explanations of the model presented in our earlier paper [28] and in Sections II and III remain valid even for other choices of the potential and couplings, since they show how to relate the general behaviour of a dynamical neutrino mass to the cosmological evolution.

## V. PARAMETER CONSTRAINTS

In the earlier sections we demonstrated that models of coupled dark energy and neutrinos could produce a detectable signature in cosmological surveys. Indeed, the modifications to the background evolution (mainly to the dark energy equation of state), temperature anisotropy spectrum and matter power spectrum should allow us to constrain our model using current data sets.

We perform our likelihood analysis using CosmoMC [70]. This program uses a Markov-Chain Monte-Carlo (MCMC) engine to efficiently explore the cosmological parameter space. Typically we run five chains for each simulation, with no less than 35,000 samples per chain. We perform the usual convergence checks on the individual chains to ensure that the chains have fully sampled our parameter space. As well as visually confirming that the individual chains converge, we check the Gelman and Rubin R statistic (variance of chain means/mean of

chain variances) for each parameter, and ensure that the Raftery and Lewis convergence diagnostic is satisfied.

We take advantage of the wide range of cosmological data which is currently available to constrain our model. The CMB temperature anisotropy spectrum is constrained using WMAP [71] [72], CBI [73], ACBAR [74] and VSA [75] datasets. The neutrino–dark energy coupling can also affect the formation of large scale structure which is sensitive to the neutrino mass, and so we use data from the Sloan Digital Sky Survey [76] to further constrain our model. Data from the Supernova Cosmology Project [77] can also be used to constrain the equation of state of dark energy, and thus place further constraints on our model.

We choose to perform the data analysis using our usual choice of potential and coupling, namely  $V(\phi) = V_0 e^{-\sigma\phi}$  and  $m_\nu(\phi) = M_0 e^{\beta\phi}$ . We choose to focus on these potentials because they embody the typical behaviour observed for most models of coupled neutrinos, and they easily reduce to the standard  $\Lambda$ CDM case ( $\beta = \sigma = 0$ ). These potentials also have the advantage that the initial choice of  $\phi_i$  does not affect the evolution of the cosmology, as changes to the initial choice of  $\phi$  are equivalent to rescalings of the mass parameters  $M_0$  and  $V_0$ . For general choices of potentials and couplings this useful degeneracy does not exist, as the neutrino–dark energy coupling can severely restrict the range of attractor solutions. Consequently the increased number of fine-tuned free parameters required for these models would compromise the goodness of fit compared to simpler models.

Throughout our analysis we assume a flat universe, with  $\Omega = 1$ . Initially we use the standard parameterization for our cosmological model, and vary the following parameters:  $\Omega_b h^2$ ,  $\Omega_{\text{CDM}} h^2$ ,  $h$ ,  $z_{\text{re}}$  (the redshift of reionisation),  $\Omega_\nu h^2$ ,  $n_s$  (the spectral index),  $10^{10} A_s$  (the initial scalar perturbation amplitude) and the dark energy parameters  $\sigma$  and  $\beta$ . We show the results from this initial analysis is Figure 11.

Clearly Figure 11 shows that current cosmological data places no constraints on our new coupling parameters. It is well known that the current best fit analysis of cosmological data can only place an upper limit on the mass of the neutrino, and that massless neutrinos are not excluded by most cosmological data sets. However the results presented so far in this paper require that the neutrinos having a significant mass; indeed for low mass neutrinos the effects observed in this paper become largely insignificant. Despite this, as we will show later, the strength of the neutrino coupling can still be constrained by the requirement for later time acceleration.

Current cosmological data requires that the universe contains approximately 70% of dark energy, 30% of dark matter and some minor quantities of baryons and neutrinos. In the dynamics of our model there could exist *only* one critical point able to guarantee such proportions in its vicinity (see e.g. [62]). When exactly reached, this point is characterized by the total domination of the scalar field and exists only for  $|\sigma| < \sqrt{6} \approx 2.5$ . Indeed

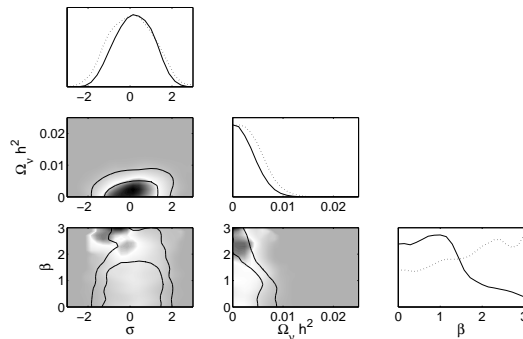


FIG. 11: Posterior constraints for 9 parameter model described in the text. Shading denotes the mean likelihood of the samples, whilst the contours show the 68% and 95% confidence limits from the marginalised distribution. Solid lines on the 1-D plots show the marginalised posterior, whilst the dotted curves denote the mean likelihood of the samples.

our computed likelihood will be shown to be contained in such boundaries. A preferred range for the parameter  $\beta$  is more difficult to predict, however, because of the previously described effects induced on the background and perturbation at different stages of the evolution, although it is clear that very large values of  $\beta$  will not be favoured by the data. But it is very important to emphasize that values of  $\beta$  of the order of unity are perfectly acceptable.

Another consideration when choosing the scalar field parameters is the BBN constraint resulting from the early time modification of the scale factor evolution due to the presence of dark energy [34, 38]. As discussed earlier, the neutrino coupling to dark energy in our model does not modify the energy density of the dark energy at the time of BBN (when the neutrinos are highly relativistic, and the coupling terms are negligible). For a quintessence potential with a scalar field dominated late time attractor the BBN constraints of [38] are easily satisfied. We have confirmed this numerically for our coupled models (for instance, in the case of  $\beta = 1$ ,  $\Omega_\phi \sim 10^{-25}$  at  $z \sim 10^8$ ). Note that, in principle, our parameter space includes both the late-time attractor and scaling solutions (that evolve like radiation or matter and which would provide a non-negligible contribution to the energy density at the time of BBN). We find, however, that the scaling solution for the exponential potential is already strongly disfavored by the observations that we have used for our analysis and therefore additional BBN constraints would not modify our findings.

Recent works [78] have used data from X-ray clusters to reduce the uncertainties on the lower bound for the neutrino mass, finding a value for the neutrino masses of  $\sum m_\nu = 0.56_{-0.26}^{+0.30}$  eV. Notice though that the upper bounds could in fact go up to  $\sum m_\nu = 2$  eV, depending on the datasets used and the assumed priors [79]. Measurements of atmospheric neutrino oscillations suggest that there is at least one neutrino species with

Parameter	Mean likelihood	68% interval	95% interval
$\Omega_{\text{CDM}}h^2$	$0.102 \pm 0.004$	$0.099 - 0.106$	$0.096 - 0.110$
$z_{\text{re}}$	$17.6 \pm 3.7$	$16.0 - 19.8$	$10.7 - 23.2$
$\sigma$	$0.43 \pm 0.32$	$0.29 - 0.60$	$0.13 - 0.95$
$\beta$	$0.75 \pm 0.64$	$0.64 - 0.98$	$0.11 - 1.18$
$n_s$	$0.96 \pm 0.01$	$0.95 - 0.97$	$0.93 - 0.99$

TABLE I: Marginalised parameter constraints for our 6 parameter model with fixed  $m_\nu = 0.2$  eV,  $\Omega_b h^2 = 0.022$  and  $h = 0.72$ . For this model we find  $\chi^2/\text{dof} = 1570.1/1459$ . This compares with a  $\chi^2/\text{dof} = 1610.1/1461$  for a best-fit  $\Lambda\text{CDM}$  model using the same parameter set with  $\sigma = \beta = 0$ .

$m_\nu > 0.05$  eV [49]. The Heidelberg-Moscow experiment, searching for neutrino-less double beta decay claim detection of electron neutrino mass  $m_{\nu_e}$  between 0.2 eV and 0.6 eV, with best fit  $m_{\nu_e} = 0.36$  eV [80].

We therefore choose to perform our analysis using two values of the neutrino mass today,  $m_\nu = 0.2$  eV and  $m_\nu = 0.3$  eV, to investigate whether models of neutrino–dark energy coupling could in principle be constrained if neutrinos were independently confirmed to have a significant ( $m_\nu \gtrsim 0.1$  eV) mass, consistent with current experiments measuring the neutrino mass.

By choosing to fix the value of the neutrino mass today, we are required to specify the current value for the energy density stored in neutrinos and value of the Hubble constant as the neutrino mass, the critical energy density in neutrinos and the Hubble constant are related via the usual formula

$$\Omega_\nu h^2 = \frac{\sum m_\nu}{93.2 \text{ eV}}. \quad (37)$$

We also choose to fix the value of  $\Omega_b h^2$  as we do not expect the behaviour and constraints of the baryon energy density to be significantly modified by our neutrino–dark energy coupling, as the observed effects on the anisotropy spectrum are largely limited to relatively low multipoles.

The values for  $H_0$  and  $\Omega_b h^2$  can be determined independently from the cosmological data used in our MCMC analysis. The value of  $H_0 = 72 \text{ km s}^{-1} \text{ Mpc}^{-1}$  can be obtained from the best fit of the Hubble Space Telescope Key Project [81], whilst the baryon density parameter  $\Omega_b h^2 = 0.022$  is favoured by Big Bang Nucleosynthesis models [82]. We are therefore left with a cosmological model requiring 6 parameters:  $\beta$ ,  $\sigma$ ,  $\Omega_{\text{CDM}}h^2$ ,  $z_{\text{re}}$ ,  $A_s$  and  $n_s$ .

The results of the MCMC analysis for neutrinos with a mass today of  $m_\nu = 0.2$  eV can be found in Table I, whilst the results for  $m_\nu = 0.3$  eV are given in Table II. We quote the marginalised probability distributions and confidence intervals. Figures 12 & 13 show the 2D probability distributions for the  $m_\nu = 0.2$  eV and  $m_\nu = 0.3$  eV models respectively.

As expected, the neutrino coupling has little effect on

Parameter	Mean likelihood	68% interval	95% interval
$\Omega_{\text{CDM}}h^2$	$0.100 \pm 0.003$	$0.097 - 0.104$	$0.094 - 0.107$
$z_{\text{re}}$	$20.5 \pm 3.1$	$19.4 - 22.0$	$15.0 - 25.1$
$\sigma$	$0.52 \pm 0.29$	$0.40 - 0.67$	$0.00 - 0.97$
$\beta$	$0.62 \pm 0.21$	$0.58 - 0.74$	$0.15 - 0.86$
$n_s$	$0.97 \pm 0.01$	$0.96 - 0.99$	$0.95 - 1.00$

TABLE II: Marginalised parameter constraints for our 6 parameter model with fixed  $m_\nu = 0.3$  eV,  $\Omega_b h^2 = 0.022$  and  $h = 0.72$ . In this case we find  $\chi^2/\text{dof} = 1593.7/1459$ . This compares with a  $\chi^2/\text{dof} = 1636.8/1461$  for a best-fit  $\Lambda\text{CDM}$  model using the same parameter set with  $\sigma = \beta = 0$ .

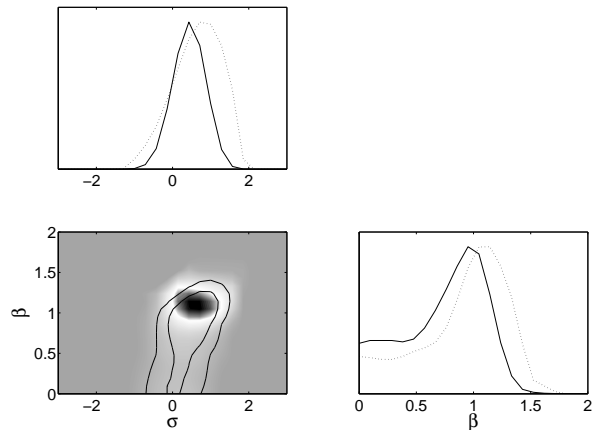


FIG. 12: Posterior constraints for 6 parameter model, with  $m_\nu = 0.2$  eV,  $\Omega_b h^2 = 0.022$  and  $h = 0.72$ . Shading denotes the mean likelihood of the samples, whilst the contours show the 68% and 95% confidence limits from the marginalised distribution. Solid lines on the 1-D plots show the marginalised posterior, whilst the dotted curves denote the mean likelihood of the samples.

the value of  $\Omega_{\text{CDM}}h^2$  as the peak structure of the temperature anisotropy spectrum is largely unaffected. The value found for  $n_s$  is also within the usual range for parameter analysis of cosmological models which neglect tensor contributions.

For both the  $m_\nu = 0.2$  eV and  $m_\nu = 0.3$  eV models we find that non-zero values of neutrino coupling strengths are preferred by the data. We also see that for these models a non-zero value for  $\sigma$  is preferred over the usual cosmological constant, although  $\sigma = 0$  is not excluded at the 68% level. This is not surprising since we have seen that the equation of state of the dark energy for some choices of parameters in our coupled models is entirely consistent with the preferred value of  $w_{\text{ap}} \sim -1$  found from supernova surveys. It is clear that models with heavier neutrinos allow stronger constraints to be placed upon the strength of the coupling. Indeed, for the 0.3 eV neutrinos we find that neutrino–dark energy coupling is

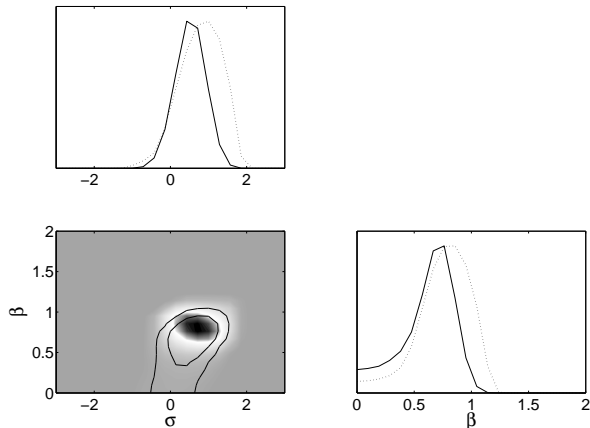


FIG. 13: Posterior constraints for 6 parameter model, with  $m_\nu = 0.3$  eV,  $\Omega_b h^2 = 0.022$  and  $h = 0.72$ . Shading denotes the mean likelihood of the samples, whilst the contours show the 68% and 95% confidence limits from the marginalised distribution. Solid lines on the 1-D plots show the marginalised posterior, whilst the dotted curves denote the mean likelihood of the samples.

preferred at the 1 sigma confidence level. This is to be expected as a larger neutrino mass today is equivalent to a higher energy density in neutrinos, and so any modification to the neutrino evolution will have a larger impact on the CMB and LSS for models with greater densities of neutrinos. In particular we have seen that there exist a range of non-zero  $\beta$  values capable of reducing power at low CMB multipoles. This last effect is most probably the cause for the relative peak in the likelihood for  $\beta$  of order unity. Furthermore a sharper drop at large values of  $\beta$  is observed in the likelihood most likely to limit the excessive growth at multipoles  $10 < \ell < 100$ .

It is however important to make clear that these constraints rely upon the assumption that the neutrino mass is known, and that the neutrinos have a mass  $m_\nu \gtrsim 0.1$  eV. Although this assumption is consistent with current neutrino experiments, we can only make the statement that should the mass of the neutrino be found to be greater than 0.1 eV, then cosmological data can be used to constrain the strength of any neutrino–dark energy coupling; indeed we find that there is some evidence that the existence of such a coupling is actually preferred by current cosmological data over the standard  $\Lambda$ CDM cosmology.

## VI. CONCLUSIONS

We have investigated models of dark energy which couple a quintessence scalar field to massive neutrinos. In these models, dark energy and neutrinos are coupled such that the neutrino masses become functions of the scalar field. The effects of such models on the cosmological

background evolution, on the cosmic microwave background anisotropies, and on the formation of large scale structures were analyzed. Additionally, we have also performed a likelihood analysis on the parameter space of such theories.

We have focused on two specific models: In the first, the coupling between neutrinos and dark energy is constant and the quintessential potential is an exponential. The second model, which is better motivated from the particle physics point of view, has a neutrino–coupling which depends on the quintessence field (hence changes with time), whilst the scalar field has a power-law potential. In spite of some specific differences between these two models (such as the energy density stored in the scalar field at recombination for example), the effects of the coupling on the CMB anisotropies and on the matter power spectrum are nevertheless explainable by the basic mechanisms that we have identified earlier. Namely, the coupling modifies the background history and induces an ISW contribution to the CMB spectrum; the matter power spectrum is modified by the magnitude of the neutrino mass during structure formation. Given the generality of these explanations, the conclusions drawn from this investigation could probably be applied to any similar model with a neutrino–dark energy coupling.

It is important to note that in our models, the dark energy sector is described by a *light* scalar field, with a mass which is at most of order  $H$ . This is in contrast to previous models [18] in which the mass of the scalar field is much larger than  $H$  for most of its history. The latter can have significant effects upon the behaviour of the neutrinos and the growth of their perturbations, and which is difficult to reconcile with current astronomical data [33].

Solving the collisionless Boltzmann equation for the neutrinos, we have investigated the relativistic and non-relativistic regimes and the transition period in between. Initially the neutrinos are highly relativistic, and during this period the quintessence field is frozen. The mass of the neutrinos therefore remains constant. As the neutrinos become non-relativistic they begin to exchange energy with the quintessence field via the coupling term. At a temperature scale comparable to the neutrino mass, the neutrinos become non-relativistic, whilst the quintessence field is dominated by kinetic energy. It is at this point that the neutrino mass begins to evolve significantly. The details of this behaviour and evolution depends on the choice of the coupling  $\beta$  and the potential parameter  $\sigma$ . In fact, the masses of the neutrinos can be heavier or lighter in the past depending on the choice of potential and coupling parameters.

The coupling of neutrinos to dark energy slightly alters the evolution of the cosmological background. It was found that similarly to models with a dark matter/dark energy interaction, the apparent equation of state measured with Type Ia Supernovae at high redshift can be smaller than  $-1$ , without introducing phantom fields, and might even cross the boundary  $w = -1$ .

The most obvious modifications to the CMB anisotropy spectrum occur for large angular scales, with  $\ell < 100$ , where the dominant contribution to the anisotropies is generated by the Integrated Sachs-Wolfe Effect (IWS). This arises due to the evolution of the gravitational potentials along the photon path from the surface of last scattering. The modification to the cosmological background arising from the neutrino coupling can also have a significant effect upon the evolution of the perturbations. We generally observe an increase in power for  $10 < \ell < 100$ , whilst for  $\ell < 10$  we find either an excess or reduction in power depending upon our choice of parameters. For the models where the neutrinos were much heavier in the past than today, we also observe a slight shift in the peaks and a modification in their relative amplitude.

The matter power spectrum exhibits free-streaming damping even in the presence of dark energy–neutrino coupling. However, since the damping scale is mainly dependent on the value of the neutrino mass at the end of their relativistic stage, our results appear similar to the standard models with CDM and hot dark matter in which the mass is fixed at the relativistic plateau. It is obvious that the mass inferred from the damping of the matter power spectrum is, in general, different from the neutrino mass measured with experiments in the laboratory.

We performed a likelihood analysis using SNIa, CMB and LSS datasets. Initially, we used the standard parameterization for our cosmological model, characterized by exponential dependence of the dark energy potential and neutrino mass on the scalar field. For a flat universe we varied all of the matter parameters, the Hubble constant, the initial power spectrum spectral index and amplitude and the instantaneous reionization parameter  $z_{\text{re}}$ . As expected, the cosmological data did not place strong constraints on our new coupling parameters. This is no surprise, since it is well known that the current best fit analysis of cosmological data can only place an upper limit on the mass of the neutrino, and a zero neutrino mass is not excluded by most cosmological data sets. An interesting outcome was that couplings of order unity are perfectly acceptable with the actual data.

To proceed, we chose to perform an analysis using two values of the neutrino mass today,  $m_\nu = 0.2$  eV and  $m_\nu = 0.3$  eV, to investigate whether models of neutrino–dark energy coupling could in principle be constrained if neutrinos were independently confirmed to have a significant mass ( $m_\nu \gtrsim 0.1$  eV), consistent with current experiments.

For both the  $m_\nu = 0.2$  eV and  $m_\nu = 0.3$  eV models we found that non-zero values of neutrino coupling strengths of order unity are preferred by the data. We also saw that for these models a non-zero value for  $\sigma$  is preferred over the usual cosmological constant, although  $\sigma = 0$  is not excluded at the 68% level. Models with heavier neutrinos allow stronger constraints to be placed upon the strength of the coupling. Indeed, for the 0.3 eV neutrinos we found

that neutrino–dark energy coupling is preferred at the 1 sigma confidence level.

One should note that these constraints rely upon the assumption that the neutrino mass is known, and that the neutrinos have a mass  $m_\nu \gtrsim 0.1$  eV. Although this assumption is consistent with current neutrino experiments, we can only make the statement that should the mass of the neutrino be found to be greater than 0.1 eV, then current cosmological data can be used to constrain the strength of any neutrino–dark energy coupling.

### Acknowledgments

We are grateful to S. Bridle, O. Elgaroy, H. K. Eriksson, F.K. Hansen, D. Hooper, A. Melchiorri, J. Silk, C. Skordis and J. Weller for useful discussions. We also thank A. Lewis for allowing us to use his CAMB quintessence module. AWB is supported by PPARC. DFM acknowledge support from the Research Council of Norway through project number 159637/V30. DTV acknowledges a Scatcherd Scholarship.

### Erratum

The original version of this paper contained a typo and a mistake, as noted by [83]. This section contains the corrected equations and Figures, as published in our Erratum [84].

The geodesic equation (23) contains a typo and should read

$$P^0 \frac{dP^\rho}{d\tau} + \Gamma_{\alpha\beta}^\rho P^\alpha P^\beta = -m_\nu^2 \frac{d \ln m_\nu}{d\phi} \frac{\partial \phi}{\partial x_\rho}, \quad (38)$$

A subtle error occurred in eq. (24), which should read

$$\frac{dq}{d\tau} = -\frac{1}{2} q \dot{h}_{ij} n_i n_j - a^2 \frac{m_\nu^2}{q} \frac{\partial \ln m_\nu}{\partial \phi} \frac{\partial \phi}{\partial x^i} \frac{\partial x^i}{d\tau}. \quad (39)$$

It follows that a scalar field dependent term should be included in the Boltzmann equation (26), giving:

$$\begin{aligned} \frac{\partial \Psi}{\partial \tau} + i \frac{q}{\epsilon} (\mathbf{k} \cdot \mathbf{n}) \Psi + \frac{d \ln f_0}{d \ln q} \left[ \dot{\eta} - \frac{\dot{h} + 6\dot{\eta}}{2} (\mathbf{k} \cdot \mathbf{n})^2 \right] \\ = i \frac{q}{\epsilon} (\mathbf{k} \cdot \mathbf{n}) k \frac{a^2 m_\nu^2}{q^2} \frac{\partial \ln m_\nu}{\partial \phi} \frac{d \ln f_0}{d \ln q} \delta \phi \end{aligned} \quad (40)$$

Therefore, the dipole equation for the neutrino hierarchy derived in [57] is subject to a change represented by a new term once again dependent on the scalar field:

$$\dot{\Psi}_1 = \frac{1}{3} \frac{q}{\epsilon} k (\Psi_0 - 2\Psi_2) - \frac{1}{3} \frac{q}{\epsilon} k \frac{a^2 m_\nu^2}{q^2} \frac{\partial \ln m_\nu}{\partial \phi} \frac{d \ln f_0}{d \ln q} \delta \phi \quad (41)$$

This modification will have an effect on the ISW effect, which is less pronounced than reported in our paper. The corrected evolution of the metric variables  $\Phi + \Psi$  is shown in Figure 14.

This will effect the anisotropies in the CMB, which are shown in Figure 15.

On the other hand, we do not find changes to the matter power spectrum or the evolution of the neutrino density contrast at the scale given in Fig. 7 in our original paper. At smaller scales we register small differences in the neutrino and scalar field density contrasts, which leads to the mentioned changes in the ISW effect. Note that the background evolution reported in [28, 85] is not affected.

We do not attempt to redo the comparison of our model with data, as the new WMAP 3-year data have been published since [86], and these models were analysed in [83].

We are grateful to K. Ichiki for correspondence. The correct equations (2)-(4) have been derived in [83].

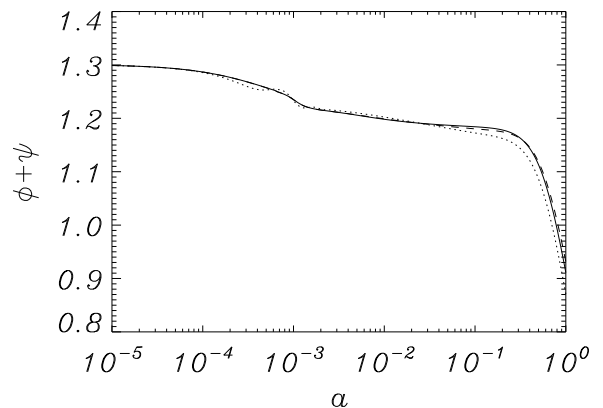


FIG. 14: Evolution of the metric variables  $\Phi + \Psi$ . Solid line:  $\beta = 0, \lambda = 1$ ; short-dashed line:  $\beta = 1, \lambda = 1$ ; dotted line:  $\beta = -0.70, \lambda = 1$ ; long-dashed line:  $\beta = 1, \lambda = 0.5$ . The scale is  $k = 10^{-3} \text{ Mpc}^{-1}$ .

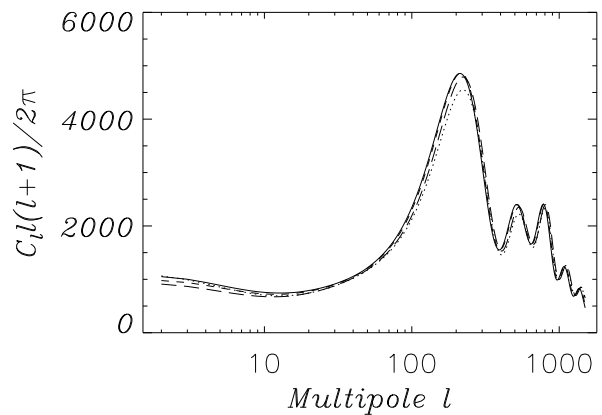


FIG. 15: The CMB anisotropy spectrum (unnormalized) for exponential coupling and potential. Solid line:  $\beta = 0, \lambda = 1$ ; short-dashed line:  $\beta = 1, \lambda = 1$ ; dotted line:  $\beta = -0.79, \lambda = 1$ ; long-dashed line:  $\beta = 1, \lambda = 0.5$ .

- 
- [1] D. Spergel et al., *Astrophys.J.Suppl.* **148**, 175 (2003)  
 [2] A. Riess et al., *Astron. J.* **116**, 1009 (1998)  
 [3] S. Perlmutter et al., *Astrophys. J.* **517**, 565 (1999)  
 [4] C. Wetterich, *Nucl. Phys. B* **302**, 668 (1988)

- [5] B. Ratra and J. Peebles, *Astrophys. Journ. Lett.* **325**, 17 (1988)  
 [6] A. Albrecht and C. Skordis, *Phys. Rev. Lett.* **84**, 2076 (2000)

- [7] C. Wetterich, *Astron.Astrophys.* **301**, 321 (1995)
- [8] M. Doran and J. Jaeckel, *Phys.Rev.D* **66**, 043519 (2002)
- [9] S.M. Carroll, *Phys.Rev.Lett.* **81**, 3067 (1998)
- [10] J.A. Frieman, C.T. Hill, A. Stebbins and I. Waga, *Phys.Rev.Lett.* **75**, 2077 (1995)
- [11] J.E. Kim and H.-P. Nilles, *Phys.Lett.B* **533**, 1 (2003)
- [12] N. Kaloper and L. Sorbo, *astro-ph/0511543*
- [13] R. Peccei in: *Sources and detection of dark matter and dark energy in the universe*, ed. David B. Cline, Springer Verlag (2001)
- [14] P.Q. Hung, *hep-ph/0010126*
- [15] M. Li, X. Wang, B. Feng and X. Zhang, *Phys.Rev.D* **65**, 103511 (2002)
- [16] M. Li and X. Zhang, *Phys.Lett.* **B573**, 20 (2003)
- [17] P. Gu, X. Wang and X. Zhang, *Phys.Rev D* **68**, 087301 (2003)
- [18] R. Fardon, A.E. Nelson and N. Weiner, *JCAP* **0410**, 005 (2004)
- [19] D.B. Kaplan, A.E. Nelson and N. Weiner, *Phys.Rev.Lett.* **93**, 091801 (2004)
- [20] P. Gu and X.-J. Bi, *Phys.Rev.D* **70**, 063511 (2004)
- [21] X. Bi, P. Gu, X. Wang and X. Zhang, *Phys.Rev.D* **69**, 113007 (2004)
- [22] H. Bi, B. Feng, H. Li and X. Zhang, *hep-ph/0412002*
- [23] E.I. Guendelman and A.B. Kaganovich, *hep-th/0411188*
- [24] H. Li, Z. Dai and X. Zhang, *Phys. Rev. D* **71**, 113003 (2005)
- [25] R.D. Peccei, *Phys.Rev.D* **71**, 023527 (2005)
- [26] P.Q. Hung and H. Pas, *Mod.Phys.Lett.* **A20**, 1209 (2005)
- [27] X.-F. Zhang, H. Li, Y. Piao and X.-M. Zhang, *astro-ph/0501652*
- [28] A.W. Brookfield, C. van de Bruck, D.F. Mota and D. Tocchini-Valentini, *Phys. Rev. Lett.* **96**:061301,2006.
- [29] V. Barger, P. Huber and D. Marfatia, *hep-ph/0502196*
- [30] M. Cirelli, M.C. Gonzalez-Garzia and C. Pena-Garay, *Nucl.Phys.B* **719**, 219 (2005)
- [31] R. Horvat, *astro-ph/0505507*
- [32] R. Barbieri, L.J. Hall, S.J. Oliver and A. Strumia, *hep-ph/0505124*
- [33] N. Afshordi, M. Zaldarriaga and K. Kohri, *Phys.Rev.D* **72**, 065024 (2005)
- [34] E. J. Copeland, A. R. Liddle and D. Wands, *Phys. Rev. D* **57** (1998) 4686
- [35] L. Amendola, *Phys. Rev. D* **62** (2000) 043511
- [36] L. Amendola and D. Tocchini-Valentini, *Phys. Rev. D* **64** (2001) 043509
- [37] P. G. Ferreira and M. Joyce, *Phys. Rev. D* **58** (1998) 023503
- [38] R. Bean, S. H. Hansen and A. Melchiorri, *Phys. Rev. D* **64** (2001) 103508
- [39] R. Takahashi and M. Tanimoto, *hep-ph/0507142*
- [40] R. Fardon, A. Nelson and N. Weiner, *hep-ph/0507235*
- [41] M. Honda, R. Takahashi and M. Tanimoto, *hep-ph/0510018*
- [42] N. Weiner and K. Zurek, *hep-ph/0509201*
- [43] V. Barger, D. Marfatia and K. Whisnant, *hep-ph/0509163*
- [44] H. Li, B. Feng, J.-Q. Xia and X. Zhang, *astro-ph/0509272*
- [45] P.-H. Gu, X.-J. Bi and X. Zhang, *hep-ph/0511027*
- [46] T. Schwetz and W. Winter, *hep-ph/0511177*
- [47] M.C. Gonzalez-Garcia, P.C. de Holanda, R.Z. Funchal, *hep-ph/0511093*
- [48] P.-H. Gu, X.-J. Bi, B.-L. Young and X. Zhang, *hep-ph/0512076*
- [49] Y. Fukuda et al., *Phys.Rev.Lett.* **81**, 1158 (1998)
- [50] Y. Ashi et al., *Phys.Rev.Lett.* **93**, 101801 (2004)
- [51] E. Aliu et al., *Phys.Rev.Lett.* **94**, 081802 (2005)
- [52] R. Kallosh, A. Linde, S. Prokushkin and M. Shmakova, *Phys.Rev.D* **66**, 123503 (2002)
- [53] J. Weller and A. Albrecht, *Phys.Rev.D* **65**, 103512 (2002)
- [54] S. Das, P.S. Corasaniti and J. Khoury, *astro-ph/0510628*
- [55] G. Huey and B.D. Wandelt, *astro-ph/0407196*
- [56] L. Amendola, M. Gasperini and F. Piazza, *JCAP09(2004)014*
- [57] C.-P. Ma and E. Bertschinger, *Astrophys. Journ.* **455**, 7 (1995)
- [58] V.F. Mukhanov, H.A. Feldman and R.H. Brandenberger, *Phys.Rep.* **215**, 203 (1992)
- [59] R. Durrer, *J.Phys.Stud.* **5**, 177 (2001)
- [60] M. Giovannini, *Int.J.Mod.Phys.D* **14**, 363 (2005)
- [61] A. Lewis, A. Challinor and A. Lasenby, *Astrophys. Journ.* **538**, 473 (2000)
- [62] D. Tocchini-Valentini and L. Amendola, *Phys.Rev.D* **65**, 063508 (2002)
- [63] J. Weller and A. Lewis, *MNRAS* **346**, 987 (2003); R. Bean and O. Doré, *Phys.Rev.D* **69**, 083503 (2004)
- [64] E.J. Copeland, A.R. Liddle and D. Wands, *Phys.Rev.D* **57**, 4686 (1998)
- [65] M. Pietroni, *Phys.Rev.D* **72**, 043535 (2005)
- [66] Ph. Brax, C. van de Bruck, A.-C. Davis and C.S. Rhodes, *Phys.Rev.D* **67**, 023512 (2003)
- [67] C.S. Rhodes, C. van de Bruck, Ph. Brax and A.-C. Davis, *Phys.Rev.D* **68**, 083511 (2003)
- [68] P.J. Steinhardt, L.-M. Wang and I. Zlatev, *Phys.Rev.D* **59**, 123504 (1999)
- [69] P. Binetruy, *Phys.Rev.D* **60**, 063502 (1999)
- [70] A. Lewis and S. Bridle, *Phys.Rev.D* **66**, 103511 (2002)
- [71] L. Verde et al., *Astrophys. J. Suppl.* **148**, 195 (2003)
- [72] G. Hinshaw et al., *Astrophys. J. Suppl.* **148** 135 (2003)
- [73] A. C. S. Readhead et al., *Astrophys. J.* **609** 498 (2004)
- [74] C.-I. Kuo et al., *Astrophys. J.* **600** 32 (2004)
- [75] C. Dickinson et al., *astro-ph/0402498*
- [76] M. Tegmark et al., *Astrophys. J.* **606** 702 (2004)
- [77] S. Perlmutter et al, *Astrophys. J.* **517** 565 (1999)
- [78] S.W. Allen, R.W. Schmidt and S.L. Bridle, *Mon. Not. Roy. Astron. Soc.* **346**, 593 (2003)
- [79] O. Elgaroy and O. Lahav, *JCAP* **0304**, 004 (2003); O. Elgaroy *et al.*, *Phys. Rev. Lett.* **89**, 061301 (2002).
- [80] L. Baudis *et al.*, *Phys. Lett. B* **407**, 219 (1997).
- [81] W.L. Freedman et al, *Astrophys. J.* **553** 47 (2001)
- [82] R.H. Cyburt et al, *Phys.Lett.* **B567**, 227 (2003)
- [83] K. Ichiki and Y.-Y. Keum, *arXiv:0705.2134*
- [84] A. W. Brookfield, C. van de Bruck, D. F. Mota and D. Tocchini-Valentini, *Phys. Rev. D* **76** 049901 (2007)
- [85] A. W. Brookfield, C. van de Bruck, D. F. Mota and D. Tocchini-Valentini, *Phys. Rev. D* **73**, 083515 (2006)
- [86] D. N. Spergel *et al.* [WMAP Collaboration], *arXiv:astro-ph/0603449*.